Integrated Model for the Acoustics of Sediments

Nicholas P. Chotiros
Applied Research Laboratories
The University of Texas at Austin, TX 78713-8029
phone: (512) 835-3512 fax: (512) 835-3259 email: chotiros@arlut.utexas.edu

Award Number: N00014-12-1-0168
http://www.arlut.utexas.edu/

LONG-TERM GOALS

Physically sound models of acoustic interaction with the ocean floor including penetration, reflection and scattering in support of MCM and ASW needs.

OBJECTIVES

The objectives are: (1) Integration of phenomenological components of the Biot plus grain contact physics models, to reconcile the physical constants and processes, with a view to reducing the number of input variables, (2) a comprehensive model for all sediment types and improved modeling of grain contact physics, and (3) the development and testing of sediment acoustic models through a series of at-sea experiments.

APPROACH

The approach may be divided according to the three objective areas:

(1) Guided by experimental results, the approach has been to extend the Biot-Stoll model to include the physics of the sand grains, particularly the stiffness of the grain-grain contact and their random variations, squirt flow in the contact region, and the change of pore fluid viscosity as a function of contact width. These extensions are needed because fluid, elastic and the Biot-Stoll poro-elastic models are unable to account for the observed frequency dependence of wave speeds, attenuations and reflection loss, found in at-sea experiments since the 1980s, particularly the ONR sponsored experiments SAX99, ASIAEX, SAX04, and SW06 [1-11]. From direct measurements and inversions, it was found that attenuation increases approximately as the second power of the frequency, at frequencies below a few kiloHertz. At higher frequencies, the rate of increase is lower but variable. The Biot-Stoll poro-elastic model goes part of the way toward explaining the measurements but it cannot match the magnitude of the wave speed dispersion and high frequency attenuation trends. In this period, the emphasis is on validation throught comparison with measurements, particularly where both shear and compressional wave properties measurements were made concurrently. Partial support for a graduate student is included to develop finite element modules for poroelastic media.

Report Documentation Page

Form Approved
OMB No. 0704-0188

1. REPORT DATE	2. REPORT TYPE	3. DATES COVERED
30 SEP 2014		**00-00-2014 to 00-00-2014**

4. TITLE AND SUBTITLE	5a. CONTRACT NUMBER
Integrated Model for the Acoustics of Sediments	5b. GRANT NUMBER
	5c. PROGRAM ELEMENT NUMBER
6. AUTHOR(S)	5d. PROJECT NUMBER
	5e. TASK NUMBER
	5f. WORK UNIT NUMBER
7. PERFORMING ORGANIZATION NAME(S) AND ADDRESS(ES) **University of Texas at Austin,Applied Research Laboratories,Austin,TX,78758**	8. PERFORMING ORGANIZATION REPORT NUMBER
9. SPONSORING/MONITORING AGENCY NAME(S) AND ADDRESS(ES)	10. SPONSOR/MONITOR'S ACRONYM(S)
	11. SPONSOR/MONITOR'S REPORT NUMBER(S)

12. DISTRIBUTION/AVAILABILITY STATEMENT
Approved for public release; distribution unlimited

13. SUPPLEMENTARY NOTES

14. ABSTRACT

15. SUBJECT TERMS

16. SECURITY CLASSIFICATION OF:			17. LIMITATION OF ABSTRACT	18. NUMBER OF PAGES	19a. NAME OF RESPONSIBLE PERSON
a. REPORT	b. ABSTRACT	c. THIS PAGE			
unclassified	**unclassified**	**unclassified**	**Same as Report (SAR)**	**14**	

(2) The approach is to develop model(s) that can represent a broad range of sediments, and smoothly transition from one type of sediment into another. This is necessary because it has been observed that ocean sediments are often inhomogeneous, paticularly in the context of high frequency acoustics. The patchy seabed concept needs to be properly developed and explored in order to assess its impact on acoustic propagation and reverberation models. Practically, all underwater sediments are porous and water-permeable, therefore compatible with poro-elastic models. Although much effort has been devoted to the modeling of the sandy sediments, there are other sediments, particularly softer sediments, in which the attenuation is proportional to the first power of frequency. The approach is to understand the physical processes in a wide range of sediment types and contruct a model that is able to accommodate them. For example, the model must be able to accommodate the frequency dependencies of the attenuation and sound speed in sandy and muddy sediments, and be capable of smoothly transitioning from one to the other, through the adjustment of a few parameters. In this reporting period, special emphasis is placed on fine-grained muddy sediments.

(3) The new model(s) are proven by comparison with archived measurements, and new measurements from at-sea experiments. The preferred approach is to isolate the bottom reflected signals and measure bottom loss, and then to use the measured bottom loss as a function of frequency and angle to invert for sediment properties. This approach allows more than one bottom model to be tested, and is less likely to be biased. In this endeavor, archival data from the SAX99, SAX04 and SW06 experiments, and new data from the Noble Mariner 12 Sea trials and the Target and Reverberation Experiment of 2013 (TREXI3) were aggregated for model validation purposes.

WORK COMPLETED

The work completed is as follows:

(1) The extended Biot (EB) model was compared to the existing shear wave measurements in the published literature. This resulted in a JASA paper in which good agreement was achieved with a wide range of published measurements. It was also instructive to compare with competing models to see where the differences lie. Although shear waves are often too slow to be efficiently coupled to compressional waves in ocean sediments, and thereofore viewed as less important in sonar applications, they are valuable in testing the validity of competing models. Model-data comparisons made using published concurrent measurements of shear and compressional wave properties are very instructive.

Under this task, a graduate student, Anthony Bonomo, was funded to work with COMSOL to develop a poroelastic module for the analysis of sound propagation using finite elements.

(2) Work continued in the expansion of the EB model to cover a wide range of sediment types. The emphasis in this period was on mud sediments. In general, they have low porosity, permeability and frame moduli. The formulation of the Biot equations needs to be such that low or zero values in any of these parameters do not cause a singularity. A set of tentative parameters were arrived at to represent muddy sediments. Variability of the sediment continues to be an issue and data previously provided by the Naval Oceanographic Office were examined in an effort to quantify the variability as a function of frequency.

(3) The main experimental component was the analysis of the data collected in the TREX13 experiment off Panama City, FL, in 2013. The equipment included a laser bottom profiler and acoustic reflection loss measurement instrument deployed on a remotely operated vehicle (ROV). In addition, there was also a collaboration with the Acoustics Research Laboratory of the National University of Singapore (ARL-NUS) to tow a thin-line array for sediment characterization purposes.

RESULTS

The results may be summarized as follows:

(1) The published measurements of wave attenuation and speed in water-saturated sand and glass beads were employed as a way to test and compare acoustic models. Although shear waves are often ignored in many applications of sediment acoustic models, they contain valuable properties that can shed light on the physical processes within. Some dry and water-saturated materials are known to follow a constant-Q model, in which the attenuation, expressed as Q^{-1}, is independent of frequency. The associated loss mechanism is thought to lie within the solid material. This model has been associated with seismic wave propagation in essentially dry soil. A second loss mechanism in fluid-saturated porous materials is the viscous loss due to relative motion between pore fluid and solid frame predicted by the Biot-Stoll model. It contains a relaxation process that makes the Q^{-1} change with frequency, reaching a peak at the characteristic frequency. Examination of the published measurements above 1 kHz, particularly those of Brunson 1983 [12], shows yet another peak, which is explained in terms of a relaxation process associated with the "squirt flow" at the grain-grain contact. In the process of deriving a model for this phenomenon, it was necessary to consider the micro-fluidic effects associated with the flow within a thin film of water confined in the gap at the grain-grain contact, and the resulting increase in the effective viscosity of water. The result is an extended Biot (EB) model that is applicable over a broad band of frequencies for both shear and compressional waves. The fitting of the EB model to the measurements of Brunson is shown in Fig. 1.

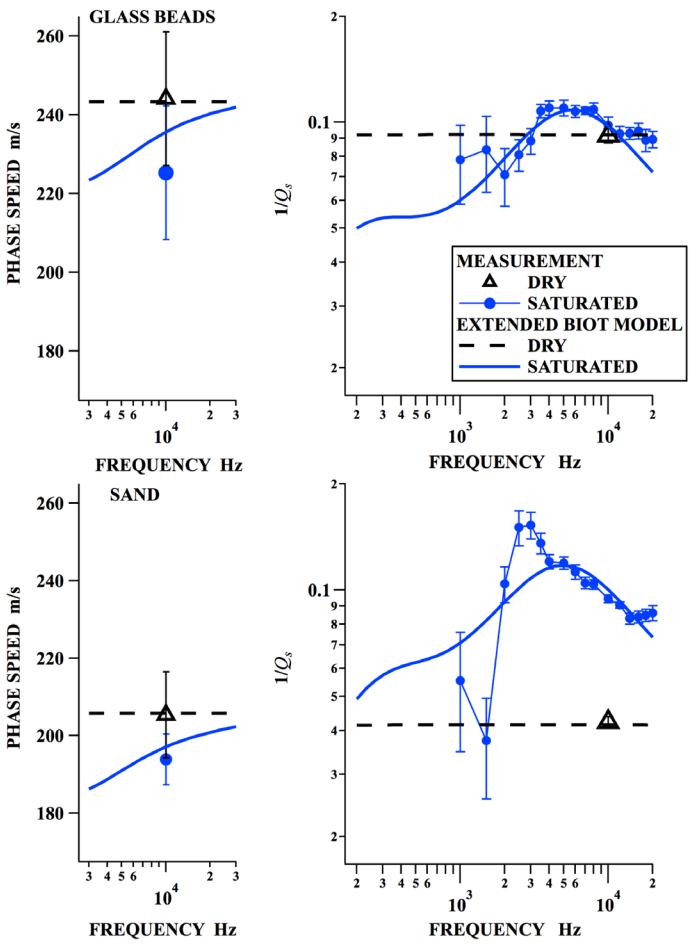

Fig. 1. Shear wave speed and attenuation as a function of frequency, in dry and water-saturated glass beads (top row) and sand (bottom row), measured by Brunson, and compared to the Extended Biot model using parameter values obtained by Brunson and frame modulus adjusted to fit. All the measured data points have bars indicating the 90% confidence intervals, although some are too small to be seen.
[The left panels show shear wave speed as a function of frequency with measured and modeled data points. The right panels show shear wave attenuation as a function of frequency. The top row of panels refer to a sample of glass beads, and the bottom to a sample of sand.]

All the measureable Biot parameters were from Brunson's dissertation [12]. The values of low frequency frame bulk moduls K_y and its relaxation frequency f_k were adjusted to fit the measured attenuation. Other models, including the Biot-Stoll [2] and grain shear models, were unable to be adjusted to fit the data, because they lacked the physical mechanisms that would allow them to follow the trend in the measured data. The mechanism in question is squirt flow at the grain-grain contact. It is the process by which a thin film of pore fluid is expelled from the grain-grain contact in the high pressure part of the acoustic cycle, and pulled back in at low pressure. It modulates the stiffness of the grain-grain contact, which controls the frame bulk and shear moduli aggregately. It also contains a loss mechanism in the viscous loss that is

incurred when fluid is expelled and pulled back. In summary, there are three identifiable loss mechanisms in this data set: the constant-Q loss mechanism within the solid material or solid part of the grain-grain contact, the viscous loss due to relative motion of the pore fluid and the skeletal frame of the Biot-Stoll model, and the viscous losses due to squirt flow. The last two involve viscous losses but they are very different in character. The Biot viscous loss is governed by the viscosity of the fluid and permeability of the skeletal frame. The squirt flow viscous loss, it was deduced, is governed by a much higher viscosity, that is only found in thin water films, typically a few nanometers in thickness. In the normal flow of water, weak hydrogen-hydrogen bonds are continually made and broken as molecules slide by one another. In thin films, which are only a few molecules wide, the flow is constricted by the electrostatic forces between molecules and the surrounding solid material, which impedes free movement. The increase in viscosity is a microfluidic property, and it is an integral part of the squirt flow process.

The EB model was shown to fit concurrent measurements of shear and compressional wave speeds and attenuation published in the literature, including those by Bell[13] and Prasad [14], and the SAX99 measurements [1], as shown in the figures below. The comparison with the viscous grain shearing (VGS(λ)) [15] is an interesting one, because both models can be fitted to the measured data points from SAX99 but their behavior beyond the measured regions is quite different. A more difficult test of the VGS(λ) model is the comparison with Brunson's measurements, where the Q^{-1} value initially rises with frequency, peak and then decay. The VGS(λ) model is constrained to start at an asymptotic Q^{-1} value of 2 in the low frequency limit, and may be adjusted to fit the downward sloping part of the measured curve by the adjustment of the parameters n and τ_s, but it is quite unable to fit the rising part. This limitation is structural to the VGS(λ) model and cannot be overcome by any parameter adjustment.

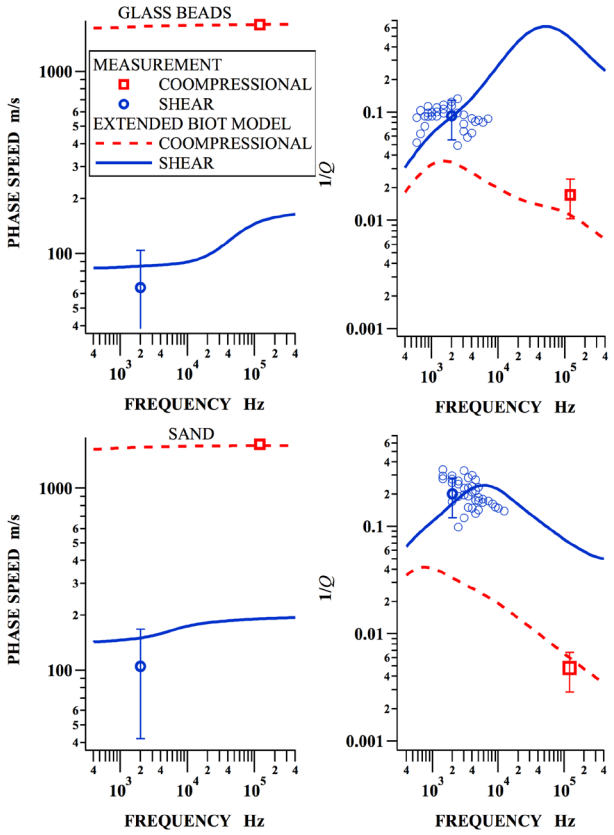

Fig. 2. Shear and compressional wave speeds and attenuations as a function of frequency, in water-saturated glass beads (top row) and sand (bottom row), measured by Bell, and compared to the EB model using parameter values measured by Bell and the adjustment of three free parameters. All the average data points have bars indicating the + and – one standard deviation limits, although some are too small to be seen. In the case of the shear attenuation, the individual measurements are also shown.

[The left panels show wave speeds as a function of frequency. The right panels show wave attenuation as a function of frequency. The top row of panels refer to a sample of glass beads, and the bottom to a sample of sand.]

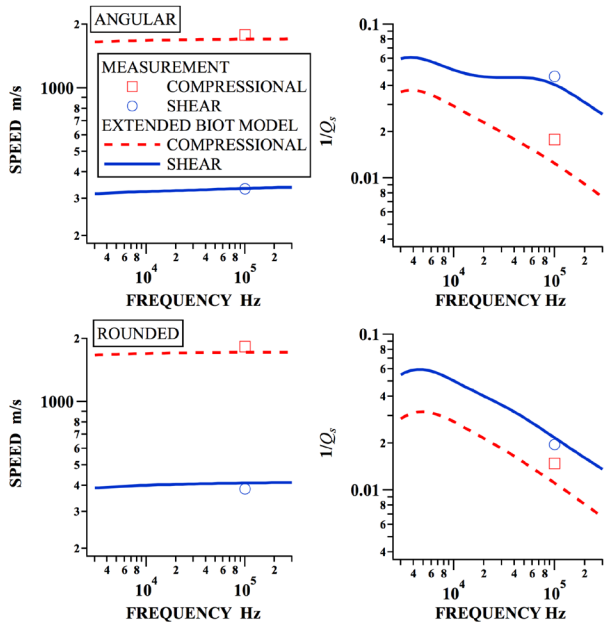

Fig. 3. Shear and compressional wave speeds and attenuations as a function of frequency, in water-saturated angular (top row) and rounded (bottom row) sand samples, measured by Prasad at an axial stress of 1 MPa, and compared to the Extended Biot model.
[The left panels show wave speeds as a function of frequency. The right panels show wave attenuation as a function of frequency. The top row of panels refer to a sample of angular sand grains, and the bottom to rounded grains.]

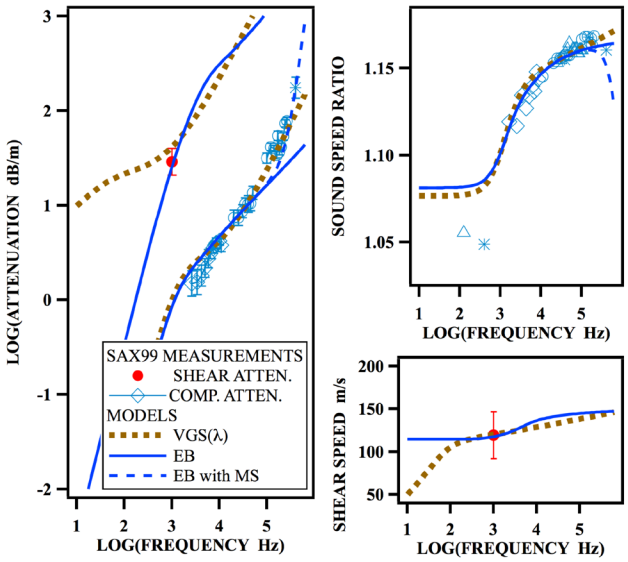

Fig. 4. Shear and compressional wave speeds and attenuations as a function of frequency measured at SAX99, and compared to the VGS(λ) and EB models, including an EB model with modification to account for multiple scattering (MS).
[The left panel shows wave attenuations as functions of frequency with measured and modeled data points. The right panels show wave speeds as a function of frequency.]

Working with COMSOL and under the joint supervision of Marcia Isakson, Anthony Bonomo, a graduate student, developed a finite element (FE) module to study the scattering of underwater sound from rough poroelastic surfaces. A number of cases were studied and compared with existing models, including the small perturbation and the Kirchhoff approximations. A comparison of monostatic scattering strengths is shown below. The work is ongoing but it is evident that the results are in agreement with existing models at small roughnesses (kh<1), where they are expected to be valid. The FE model is expected to be valid for large roughnesses and some differences are evident in the results but the reasons for the differences are unclear at this point and more investigations are in order to fully test the new model.

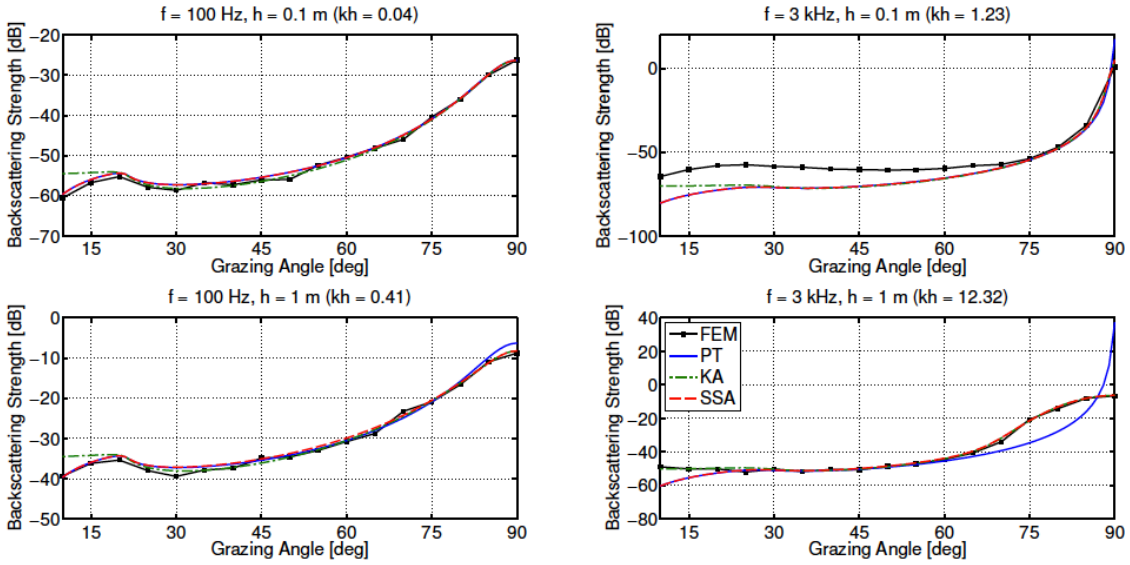

Fig. 5. Monostatic scattering strengths given by perturbation theory (PT), the Kirchhoff approximation (KA), the small-slope approximation (SSA), and the finite element method (FEM) for four cases.
[The left and right panels show results at a frequency of 100 and 3000 Hz, respectively. The kh values increase from top to bottom and from left to right.]

(2) The application of the EB model to cover a wide variety of sediment types was continued with emphasis on muddy, fine grained sediments, in preparation for the Sediment Characterization experiment, which will have a significant muddy sediment component. A starting point is the set of model parameters that were developed to match the sediment types within the APL-UW model sediments known as HFEVA. The sound speed, attenuation and normal reflection loss curves as a function of frequency are shown in Fig. 6. The fine-grained sediments are the green curves with grain diameters in the 5 to 9 ϕ range. The normal reflection loss is uniformly low and it would be very difficult to distinguish one grain size from another within this group. They have sound speeds that are slightly lower than water, due to the increased density but relatively unchanged bulk modulus relative to water. The attenuation is known to increase linearly with frequency, and the model is able to accommodate this trend within a limited frequency range from 3 to 1000 kHz. Measurements or inversions below this frequency band are rather sketchy because of the extremely low attenuation. One of the key components, that permits the EB model to approximately match the linear frequency dependence of attenuation, is the

Yamamoto and Turgut [16] model for a range of pore sizes, which is assumed to be log-normal and can span several orders of magnitude. There is some physical evidence to support it. In the study of fine grained sediments from Eckernförde Bay, Bennett et al. [16] showed several transmission electron microscope (TEM) images that indicated a "heterogeneity of packing of particles and resulting distribution of pore diameters". The Yamamoto and Turgut model provides a direct connection between the distribution of pore sizes and the approximately linear dependence of attenuation on frequency.

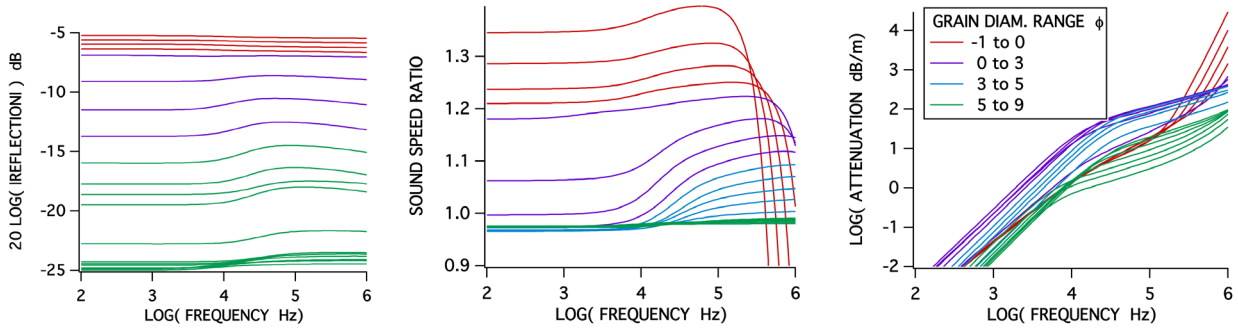

Fig. 6. The EB equivalent of HFEVA sediment model, in the form of normal reflection (left), sound speed (middle) and attenuation (right) as functions of frequency.
[The frequency scale ranges from 100 Hz to 1 MHz.]

Fig. 8 TEM photomicrograph of Eckernförde Bay sediment (sample depth 1 mm) showing heterogeneity of packing of particles and resulting distribution of pore diameters

Fig. 7. Reproduced from Ref. 16, showing pore size distribution in a fine-grain sediment that is likely responsible for the linear frequency dependence of attenuation.
[The micrograph shows a round microbial cell surrounded by play platelets.]

(3) Laser profiling and acoustic reflection measurements were performed at the TREX13 experiment. Analysis of the laser profiles is still in process. There were problems with automatic tracking of the laser lines. A couple of undergraduate students worked on the problem and made significant improvements through the summer of 2014. The new crossed laser lines configuration has a number of pros and cons. The cons are mainly associated with the difficulty of automatic tracking and identifying laser lines in the vicinity of intersections. The pros include the ability to perform in-situ calibration verification using the positions of the intersections. New techniques were developed to use the latter extensively to refine the laser calibration in the post-processing stage and improve the accuracy of the roughness measurement.

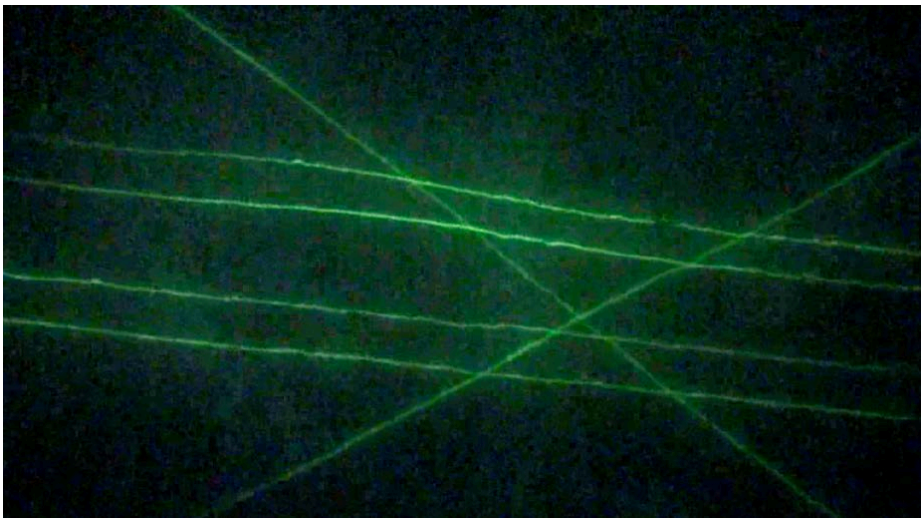

Fig. 8. Example of a video frame showing crossed laser profiler lines. [The laser lines are shown as green curvy lines on a black background.]

Analysis of the acoustic reflection data has shown the bottom to be patchy particularly in the areas designated as transition zones. These are regions that appeared to have a lower and more variable scattering strength when viewed through a 200 kHz multibeam sonar survey map. These zones were explored using the laser profiler and acoustic reflection measurement system on board the ARL:UT ROV. An example of the ROV track over transition zone 4 is shown below. The precision positioning was achieved with the aid of a Tracklink 1500 USB navigation transponder, linked to the ship's GPS positioning system.

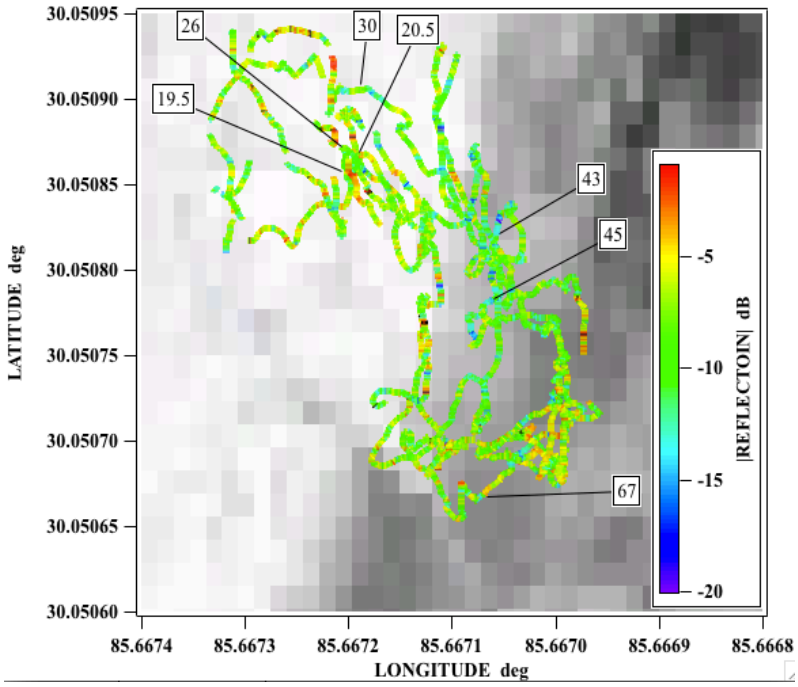

Fig. 9. ROV track and measured normal reflection loss as a function of position superimposed on the backscattering strength from the high-frequency multibeam survey at transition zone 4. The tagged numbers indicate time in minutes after start of the deployment.
[The reflection coefficient along the ROV track is color coded.]

The normal reflection loss shows rapid changes as a function of position. The example in Fig. 10 shows the variations as a function of time. Since the ROV was moving at a speed of approximately 0.5 m/s, it is evident that the reflection loss was changing on the scale of a few meters. For example, the distance between the minimum in reflection loss at 45.5 minutes to the maximum at 45.9 minutes is approximately 10 m. There appears to be a layer under the maximum with a pinch off at approximately 45.6 minutes. It is likely that the maximum is due to a patch of sand, and the areas with lower reflection are muddy fine-grained sediments.

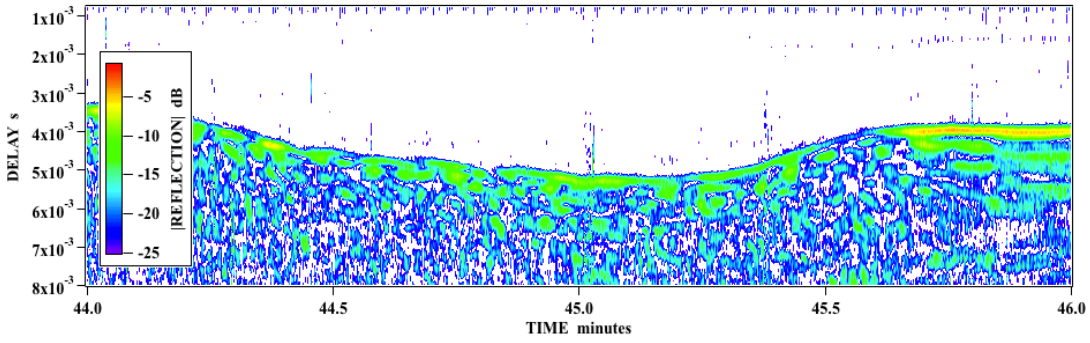

Fig. 10. Normal reflection loss along a small section of the ROV track at 45 minutes into the deployment, showing variability and fine layering.
[There is a patch of reflectivity material that is consistent with sand on the right hand side. Other parts of the track show variable reflectivity. The undulation is a consequence of the ROV height above bottom changing. The bottom was in fact very flat.]

IMPACT/APPLICATIONS

The results will impact Navy underwater acoustic propagation models, particularly where reflection and penetration of sound at the seabed are concerned. It will also impact the future structure of oceanographic databases maintained by Navy offices, including the Naval Oceanographic Office (NAVO). Predictions of sediment wave speeds and attenuations will need to be revised. In addition, the spatial variability of sediment properties will impact the accuracy of sonar performance models.

TRANSITIONS

Work on sediment variability is being transitioned to the active sonar trainers via the High-Fidelity Active Sonar Training (HiFAST) project and to future projects to improve the HFBL database. Some aspects of the ocean sediment model, particularly the frequency dependence of sediment attenuation, have been used in the Ocean Bottom Characterization Initiative (OBCI) project. This work will be used in the new project titled “Seafloor Spatial Variability Mitigation” funded by SPAWAR, for the benefit of NAVO.

RELATED PROJECTS

This project is closely related to most projects under the ONR Underwater Acoustics: High Frequency Sediment Acoustics and Shallow Water Thrusts, especially through the TREX13 experiment (www.trex13.info).

REFERENCES

1. K. L. Williams, D. R. Jackson, E. I. Thorsos, D. Tang, and S. G. Schock. "Comparison of sound speed and attenuation measured in a sandy sediment to predictions based on the Biot Theory of porous media," IEEE J. Oceanic Eng. 27, 3, 413-428, (2002).
2. R. D. Stoll. "Velocity dispersion in water-saturated granular sediment," J. Acoust. Soc. Am. 111, 2, 785-793, (2002).
3. M. A. Zimmer, L. D. Bibee, and M. D. Richardson. "Measurement of the frequency dependence of the sound speed and attenuation of seafloor sands from 1 to 400 kHz " IEEE J. Oceanic Eng. 35, 3, 538-557, (2010).
4. P. C. Hines, J. C. Osler, J. Scrutton, and A. P. Lyons. "Time-of-flight measurements of acoustic wave speed in sandy sediments from 0.6 – 20 kHz," Boundary Influences In High Frequency, Shallow Water Acoustics, N.G.Pace and P Blondel, (Eds), University of Bath, UK 5th-9th September 2005, 49-56, (2005).
5. B. T. Hefner, D. R. Jackson, K. L. Williams, and E. I. Thorsos. "Mid- to High-Frequency Acoustic Penetration and Propagation Measurements in a Sandy Sediment," IEEE J. Oceanic Eng. 34, 4, 372-387, (2009).
6. A. J. Goff, B. J. Kraft, L. A. Mayer, S. G. Schock, C. K. Sommerfield, H. C. Olson, S. P. S. Gulick, and S. Nordfjord. "Seabed characterization on the New Jersey middle and outer shelf: correlatability and spatial variability of seafloor sediment properties," Marine Geology 209, 147-172, (2004).

7. D. P. Knobles, P. S. Wilson, J. A. Goff, and S. E. Cho. "Seabed acoustics of a sand ridge on the New Jersey continental shelf," J. Acoust. Soc. Am. EL 124, 3, EL 151-156, (2008).

8. C.-F. Huang, P. Gerstoft, and W. S. Hodgkiss. "Effect of ocean sound speed uncertainty on matched-field geoacoustic inversion," J. Acoust. Soc. Am. EL 123, 6, EL162-EL168, (2008).

9. Y.-M. Jiang, and N. R. Chapman. "Bayesian geoacoustic inversion in a dynamic shallow water environment," J. Acoust. Soc. Am. 123, 6, EL155 - EL161, (2008).

10. G. R. Potty, J. H. Miller, P. S. Wilson, J. F. Lynch, and A. Newhall. "Geoacoustic inversion using combustive sound source signals," J. Acoust. Soc. Am. 124, 3, EL146-EL150, (2008).

11. M. S. Ballard, and K. M. Becker. "Geoacoustic inversion on the New Jersey Margin: Along and across the shelf," J. Acoust. Soc. Am. 124, 3, EL141-EL145, (2008).

12. B. A. Brunson. Shear wave attenuation in unconsolidated laboratory sediments, Ph. D. Thesis, Oregon State University, Corvalis, 1983.

13. D. W. Bell. Shear wave propagation in unconsolidated fluid saturated porous media, Technical Report ARL-TR-79-31, Applied Research Laboratories, The University of Texas at Austin, 1979.

14. M. Prasad. Experimental and theoretical considerations of attenuation and velocity interactions with physical parameters in sands, Ph. D. Thesis, der Mathematisch-Naturwissenschaftlichen Fakultät der Christian-Albrechts-Universität, Christian-Albrechts-Universität, Kiel, 1988.

15. M. J. Buckingham. "Response to “Comments on ‘Pore fluid viscosity and the wave properties of saturated granular materials including marine sediments [J. Acoust. Soc. Am. 127, 2095–2098 (2010)]’ ”," J. Acoust. Soc. Am. 127, 2099-2102, (2010).

16. T. Yamamoto, and A. Turgut. "Acoustic wave propagation through porous media with arbitrary pore size distributions," J. Acoust. Soc. Am. **83**, 1744-1751, (1988).

17. R. H. Bennett, M. H. Hulbert, M. M. Meyer, D. M. Lavoie, K. B. Briggs, D. L. Lavoie, R. J. Baerwald, and W. A. Chiou. "Fundamental response of pore-water pressure to microfabric and permeability characteristics: Eckernförde Bay," Geo-Marine Letters **16**, 182-188, (1996).

PUBLICATIONS

1. N. P. Chotiros and M. J. Isakson, "Shear wave attenuation and micro-fluidics in water-saturated sand and glass beads," J. Acoust. Soc. Am., vol. 135, pp. 3264-3279, 2014. [published, refereed]

2. N. P. Chotiros and M. J. Isakson, "Sediment acoustics: The need for improvement," presented at the UA2014 - 2nd International Conference and Exhibition on Underwater Acoustics, Rhodes, Greece, 2014, pp. 743-750. [published]

3. N. P. Chotiros, M. J. Isakson, J. N. Piper, and A. R. McNeese, "Sea floor roughness measured by a laser profiler on a ROV," presented at the Oceans 2014, Taipei, Republic of China, 2014. [published]

4. N. P. Chotiros and M. J. Isakson, "The high frequency environmental acoustics sediment model in the light of recent advances," J. Acoust. Soc. Am., vol. 134, p. 4207, 2014. [published]

5. A. L. Bonomo, M. J. Isakson, and N. P. Chotiros, "Comparison of the finite element method with perturbation theory and the small-slope approximation for acoustic scattering from one-dimensional rough poroelastic surfaces " J. Acoust. Soc. Am., vol. 134, p. 4251, 2013. [published]

6. A. L. Bonomo, M. J. Isakson, and N. P. Chotiros, "Acoustic scattering from a sand layer and rock substrate with rough interfaces using the finite element method," J. Acoust. Soc. Am., vol. 135, p. 2298, 2014. [published]

7. N. P. Chotiros, M. J. Isakson, J. N. Piper, and A. R. McNeese, "Spatial variation of seabed acoustic bulk properties," J. Acoust. Soc. Am., vol. 135, p. 2231, 2014. [published]